

AperTO - Archivio Istituzionale Open Access dell'Università di Torino

**Electrocatalytic reduction of CO<sub>2</sub> by thiophene-substituted rhenium(I) complexes and by their polymerized films**

**This is the author's manuscript**

*Original Citation:*

*Availability:*

This version is available <http://hdl.handle.net/2318/1591482> since 2017-01-19T22:23:00Z

*Published version:*

DOI:10.1039/C5DT04491J

*Terms of use:*

Open Access

Anyone can freely access the full text of works made available as "Open Access". Works made available under a Creative Commons license can be used according to the terms and conditions of said license. Use of all other works requires consent of the right holder (author or publisher) if not exempted from copyright protection by the applicable law.

(Article begins on next page)

This is the author's final version of the contribution published as:

Sun, Cunfa; Prosperini, Simona; Quagliotto, Pierluigi; Viscardi, Guido; Yoon, Sam S.; Gobetto, Roberto; Nervi, Carlo. Electrocatalytic reduction of CO<sub>2</sub> by thiophene-substituted rhenium(I) complexes and by their polymerized films. DALTON TRANSACTIONS. 45 pp: 14678-14688.  
DOI: 10.1039/C5DT04491J

The publisher's version is available at:

<http://pubs.rsc.org/en/content/articlepdf/2016/DT/C5DT04491J>

When citing, please refer to the published version.

Link to this full text:

<http://hdl.handle.net/2318/1591482>

# Electrocatalytic Reduction of CO<sub>2</sub> by Thiophene-substituted Rhenium(I) Complexes and by their Polymerized Films†

Cunfa Sun,<sup>a</sup> Simona Prosperini,<sup>a</sup> Pierluigi Quagliotto,<sup>a</sup> Guido Viscardi,<sup>a</sup> Sam S. Yoon,<sup>b</sup> Roberto Gobetto<sup>a</sup> and Carlo Nervi<sup>a\*</sup>

Three novel thiophene substituted bipyridine ligands and their corresponding rhenium complexes were synthesized and tested for the electrocatalytic reduction of CO<sub>2</sub>. Two complexes underwent oxidative electropolymerization on glassy carbon electrode (GCE) surface. The conductive polymers chemically deposited on GCE allow electron transport from the surface to the polymer-attached rhenium catalytic center in contact with the solution. The chemically modified electrodes show significant catalytic activities for CO<sub>2</sub> reduction, and moderate relative higher stabilities when compared with the homogeneous solution counterparts.

## Introduction

The photoelectrochemical conversion of CO<sub>2</sub> into valuable chemicals/fuels is an ideal approach for the contemporary challenges of greenhouse emission and energy shortage. However, the knowledge and technology are still in their infancy, when compared to the water splitting ones.<sup>1-6</sup> Over the last decades, many organometallic catalysts were explored for efficient and selective electrochemical CO<sub>2</sub> conversion.<sup>7-15</sup> Rhenium chlorotricarbonyl complexes bearing bipyridyl ligands introduced by Lehn<sup>16</sup> are among the most studied, robust and higher selective catalysts for the electrochemical reduction of CO<sub>2</sub> to CO.<sup>17-19</sup> The effects of several type of substituted bipyridines<sup>17, 20-23</sup> were tested, and the photochemical and electrochemical mechanism leading to CO thoroughly explored (see<sup>14, 23</sup> for a recent brief synopsis).

Most of the published papers focused on homogeneous catalysis, mainly because the design, fine-tuning and the synthesis of catalysts are more straightforward and simple. On the other hand, large-scale applications of heterogeneous catalytic systems are widespread due to their advantages in terms of operation, cost, durability and easier recovering procedure. The combination of the two approaches could make the heterogeneous CO<sub>2</sub> conversion by green energy (i.e. solar energy) more industrially feasible and appealing.<sup>18, 24</sup>

Not many papers<sup>18, 25-34</sup> deal with electrode modified by Re-bipyridine complexes, meanwhile immobilization of intact organometallic catalysts on a surface<sup>35</sup> is a challenging opportunity<sup>35-37</sup> because of potential improved stability, durability, handling and reactivity in electrochemical and photoelectrochemical cells.<sup>5</sup> Cyclic Voltammetry (CV) can quickly test the catalyst activity, simply comparing the cathodic peak currents with and without CO<sub>2</sub> atmosphere. However, the evaluation of durability is time and material consuming, usually requiring exhaustive electrolysis. Herein we suggest that one or few molecular layers of catalyst deposited on the electrode surface would dramatically reduce both the required amount of catalyst and time for durability tests, since the bulk of the solution no longer renew the catalyst produced on the electrode surface by diffusion.<sup>38, 39</sup>

Direct functionalization of the electrode surface by intact organometallic fragments can be realized by oxidation<sup>35</sup> or reduction<sup>40</sup> of a complex containing amino or diazonium groups, respectively. An alternative approach is to resort to a suitable polymer as solid support for Re catalysts. In such a case, the polymer must allow the transport of electrons from the electrode surface to the polymer-bound Re centres in contact with the solution. Thiophene and polythiophene have drawn a lot of attention for their high stability and good electron conducting properties.<sup>41-45</sup> Besides thiophene, 3'-substituted terthiophene, used as polymer backbone, shows some advantages,<sup>46, 47</sup> such as less steric hindrance and higher conductivity.

In this work, bipyridines modified at 4-position with thiophene (**T**), 2,2':5',2''-terthiophene (**TT**) and 3'-ethynyl 2,2':5',2''-terthiophene (**ETT**) were synthesized, the corresponding new Re complexes (**T**)Re(CO)<sub>3</sub>Cl (**1**), (**TT**)Re(CO)<sub>3</sub>Cl (**2**) and (**ETT**)Re(CO)<sub>3</sub>Cl (**3**) obtained (see Scheme 1), and their electrochemical behaviour in homogeneous solutions studied. We evaluated the catalytic properties of the electron-conducting polymer films. Complexes **2** and **3**, bearing

Insert Scheme 1 HERE.

terthiophene units were successfully electropolymerized on the electrode surface by oxidation and their catalytic activity towards CO<sub>2</sub> reduction compared. We thought that the active metal centre in **2** could be hindered by the

organic moiety during the polymerization process, so that **3** was synthesized in order to evaluate the effect of a C≡C triple bond (an electron-conducting rigid spacer) on the overall catalytic performance.

## Results and Discussion

### Homogeneous solution.

Fig. 1 shows the CVs of complexes **1-3** in acetonitrile under Ar and in saturated CO<sub>2</sub> solutions on Glassy Carbon Electrode (GCE). These CVs can be compared afterward with those of the corresponding heterogeneous phases (see below). The electrochemical behaviour of this class of complexes under inert atmosphere is well known.<sup>16</sup> Normally, to a first reversible or quasi-reversible 1e ligand-centred reduction follows a second chemical irreversible reduction. Cl<sup>-</sup> can be released after both reductions.<sup>48,49</sup>

For complexes **1-3** the first reduction is reversible, and apparently not affected by different thiophene units. The reduction processes are diffusion-controlled (see Fig. S1 and S2), and the trend of their reduction potentials fits<sup>17</sup> with the electronic properties of the thiophenyl-substituted bipyridines (Table 1). The second reduction is generally irreversible, and chemical complications could arise after the release of Cl<sup>-</sup>.

Chemical irreversible oxidations occur between 0.75 and 1.03 V (Table 1). These processes are expected to involve the thiophene moieties, inducing their polymerization on the electrode surface.<sup>50</sup> We used DFT calculations to shed light on the nature of the redox processes.

For all complexes, HOMO-1 orbitals are centred on the metal. In the case of **1** the HOMO (involved in the oxidation) is mainly metal-centred, while in **2** and in **3** the HOMOs are centred on the thiophene moieties (Fig. S4). Thus, electro-polymerization after the first oxidation is expected to occur on **2** and **3**, but not on **1**, because in the latter complex the metal-centred oxidation avoids the thiophene activation towards the polymerization.

Furthermore, a rough estimation of the redox potentials could

Insert Fig 1 HERE

Insert Table 1 HERE

be done by DFT methods<sup>51, 52</sup> based on the calculation of the free energy with respect that of ferrocene. The overall agreement is reasonably good (Table 1), with the understandable exception of the oxidation peak potentials that are not reversible.

In a CO<sub>2</sub>-saturated solution (~0.28 M),<sup>53</sup> the current of the second reduction markedly increased, and its magnitude is related to the activity of the catalyst in the CO<sub>2</sub> reduction process. An electrochemical method to evaluate the

Insert Table 2 HERE

homogeneous catalytic rate constant (*k*) from CV data has been proposed by Savéant and co-workers.<sup>38, 39</sup> We adopted a similar method,<sup>54</sup> herein briefly reviewed. For a reversible electron-transfer process followed by a fast catalytic reaction the catalytic current (*i<sub>c</sub>*) is given by equation (1).<sup>54</sup> The peak current (*i<sub>p</sub>*) of a reversible electron transfer process with no following reactions can be expressed by the Randles-Sevcik equation (2). Thus, a very rough estimation of *k* can be obtained by the *i<sub>c</sub>* to *i<sub>p</sub>* ratio (eq. 3),

$$i_c = n_c F A [cat] \sqrt{Dk[Q]^y} \quad (1)$$

$$i_p = 0.4463 \cdot n_p^{3/2} F A [cat] \sqrt{\frac{DFv}{RT}} \quad (2)$$

$$\frac{i_c}{i_p} = \frac{n_c}{0.4463} \sqrt{\frac{RT}{F}} \sqrt{\frac{k[Q]^y}{v}} \quad (3)$$

where *n<sub>c</sub>* is the number of electrons involved in the catalyst reduction (*n<sub>p</sub>*=1), *F* the Faraday constant, *A* the electrode area, [*cat*] the catalyst concentration, *D* the diffusion coefficient of the active catalyst, [*Q*] the concentration of the substrate (in this case CO<sub>2</sub>), *y* the kinetic order of the reaction involving the substrate, and *v*

is the scan rate. Assuming a pseudo first order kinetic and a large concentration of the substrate in comparison with that of the catalyst,  $\gamma=1$ .<sup>26, 55</sup> We are aware that this is a very rough method for rate constants evaluation. However, the computed  $k$  values for reduction of  $\text{CO}_2$  (see Table 2) are comparable to those found for  $(\text{bpy})\text{Re}(\text{CO})_3\text{Cl}$ .<sup>14, 17, 28, 29</sup>

### Heterogeneous measurements

Upon thiophene-centred<sup>50</sup> oxidation at a moderate positive potential (around 1 V, Table 1), the formation of a conductive film via electro-polymerization<sup>56</sup> of the complex is expected. The films deposited on the electrode surface were obtained going towards positive potentials by repeated CV scans (Fig. 2) at 0.2 V/s. The CV switching potentials are 0.1 V more positive than the peak potentials at 1.03, 0.88 and 0.75 V vs.  $\text{Fc}/\text{Fc}^+$  for complexes **1**, **2** and **3**, respectively. The CV of a solution of **1** is almost unchanged after several cycles (Fig. 2a). As predicted by DFT calculations, the oxidation of **1** is metal-centred and does not involve the thiophene moiety, thus no film is formed. The CV of a solution of **2** (and **3**) shows an increment of the anodic peak current at increasing number of CV cycles, indicating the formation and grow of a polymer. A new oxidation peak, assigned to a redox process of the

Insert Fig 2 HERE

polymer,<sup>27, 47, 57</sup> appears at less positive potentials.

After the polymerization of **2** (and **3**), the modified electrode was washed with  $\text{CH}_3\text{CN}$  and sonicated for 3 min to release unbounded molecules. Both surface-bounded polymers produced from solutions of **2** and **3** appear to be rather stable, since they do not change their electrochemical properties even after 12h in acetonitrile. CVs of the modified electrodes in solutions containing the supporting electrolyte only, and the homogeneous solutions show quite similar responses. Compound **2** and **3** behave in a similar way, so the rest of the discussion will be focused on the electro-polymerized film obtained from complex **2** with five CV oxidation cycles (see SI for **3**).

The GCE functionalized with **2** by this method shows at the first CV cycle three peaks, two reductions and one reoxidation, at  $-1.70$  V,  $-2.00$  V and  $-1.65$  respectively (Fig. 3). These values are approximately the same as those observed in the corresponding homogeneous solutions. The first reduction peak, not discussed in the former works,<sup>27, 29</sup> vanished in the following cycles, and probably is associated either to the release of  $\text{Cl}^-$ , or to the neutralization of the polymer film after its electro-oxidation. The small cathodic peak around  $-1.2$  V is assigned to trapped charges in the layer, or to the corresponding cationic complex in which  $\text{Cl}^-$  is replaced by MeCN.<sup>56, 57</sup>

From the second/third CV cycle, the surface-modified electrode reach a steady state, showing a stable and broad peak (green curve in Fig. 3). At higher CV scan rates two reversible processes (at  $-1.70$  and  $-2.05$  V) become evident (Fig. 4; note the same values of cathodic and anodic peaks due to the absence of diffusion). Apparently, the surface-modified electrode not only retains a very similar electrochemical behaviour of the corresponding homogeneous solution, but it seems more reversible, probably due to the effect of immobilization. Similar stabilization effect has been already observed in the case of vinylterpyridinyl complex of cobalt.<sup>58</sup>

Actually, the plot of peak current versus the CV scan rate is linear (Fig. 5), strongly suggesting that the redox process is no longer diffusion controlled, but it is associated to a bound species on the electrode surface. Dahms<sup>59</sup> and Ruff<sup>60-62</sup> showed that the diffusion coefficient in polymeric films has two main contributions, one arising from the physical diffusion of the species and a second due to electron self-exchange. However, in modified electrodes the latter term should be dominant. Since the thickness of the film in our case is very thin, the CV should be as that of an adsorbed specie on the electrode surface, with the peak current given by:<sup>63</sup>

$$i_p = \frac{n^2 F^2}{4RT} \nu A \Gamma \quad (\text{a})$$

$$i_p = \frac{\alpha F^2}{2.718RT} \nu A \Gamma \quad (\text{b})$$

for a reversible (a) or irreversible (b) chemical reaction.  $\Gamma$  is the surface coverage, i.e. the number of molecules bound to the surface, and  $\nu$  is the CV scan rate. The apparent area of the electrode  $A$  was estimated to be  $6.24 \text{ mm}^2$  by chronoamperometric measurements of a ferrocene solution at known concentration, in a similar way as previously described.<sup>35</sup> We will use this value thoroughly. From the slope of the linear regression of  $i_p$  vs.  $\nu$ ,  $\Gamma$  values of  $4.6 \times 10^{-10}$  and  $6.2 \times 10^{-10} \text{ mol cm}^{-2}$  for the reversible and irreversible cases, respectively, can be roughly estimated. This surface coverage is slightly larger, but of the same order of magnitude ( $3.43 \times 10^{-10} \text{ mol cm}^{-2}$ ), than

that observed for a monolayer of organometallic derivative of similar dimensions.<sup>35</sup> Thus, these data suggest that a preparative five CV oxidation cycles at 0.2 V/s creates few film layers on the electrode surface.

$\Gamma$  could be assessed<sup>35, 64</sup> also by means of the formula  $\Gamma=Q/FA$ , where  $Q$  is the charge that reduces or oxidizes the organometallic complexes on the electrode surface, evaluated by integration of the background-corrected CV response.  $\Gamma$

Insert Fig 3, 4 and 5 HERE

value computed on the CV performed at 0.2 V/s gave  $7.74 \times 10^{-10}$  mol/cm<sup>2</sup>, which is in reasonable good agreement with the above  $\Gamma$  value estimated from the peak current vs. scan rate. Following the same experimental procedure, a series of modified electrodes were prepared by applying an increasing number of CV oxidation cycles. In this case the formation of

Insert Table 3 HERE

multilayers and the random polymerization process does not allow a precise evaluation of the catalyst distribution on the surface. However, the measure of the total charge  $Q$  allows guessing the amount of the deposited reducible organometallic complex (either on the surface or embedded in the polymeric structure). As expected, the amount of the Re electro-active specie deposited on the electrode surface increases by increasing the number of CV cycles (Table 3). For example, after fifteen CV oxidation cycles the electrode surface holds  $35.30 \times 10^{-10}$  mol cm<sup>-2</sup> of electro-active catalyst. CV of the modified electrode shows in saturated CO<sub>2</sub> solutions a dramatic enhancement of the catalytic current. It increases by increasing the number of CV cycles used for functionalization (Table 3); instead, the  $i_c/i_p$  ratio decreases. This is reasonable since only the Re centres on the surface are in direct contact with the solution, and thus able to fully act as catalyst. In particular, the electrode obtained after 15 CV oxidation cycles ( $\Gamma = 35.30 \times 10^{-10}$  mol·cm<sup>-2</sup>), shows in saturated CO<sub>2</sub> solutions a catalytic current 93.2 times higher than that measured under Ar (Fig. 6). Similar results are obtained for **3**, where the  $i_c/i_p$  ratio is about 89 (Fig. S6).

However, we observed a current decrease during the subsequent CV cycles (Fig. 7), and after hundred CV cycles, almost no catalytic current is observed. Slightly worse results were obtained for **3** (Fig. S6), where the catalyst was completely deactivated after sixty CV cycles. This is the opposite of the expected effect. Since the alkyne unit in **3** usually does not interrupt the molecular electronic communication,<sup>65</sup> probably the rigid C≡C spacer either reacts with CO<sub>2</sub> or push away the metal centre from the solid polymer towards the solution, making its behaviour and stability more similar to a situation of the homogeneous solution where less stability is observed.

To shed light on the mechanism of surface catalyst depletion, we prepared another electrode functionalized with **2** (five CV cycles), and tested its stability at constant potentials under CO<sub>2</sub>. With an applied potential of -2.1 V vs. Fc (Fig. 8) the modified electrode shows an initial high current which slowly decreases, and in 75 min the catalytic activity on the surface is totally lost. This value is very similar to the lifetime that can be extrapolated from the 100 CV cycles above outlined, and similar also to that obtained from the exhaustive electrolysis of a homogeneous solution of (bpy)Re(CO)<sub>3</sub>Cl in the same conditions.<sup>14</sup> If one consider that few molecular layers of catalyst have the same lifetime of a whole homogeneous solution with a much higher amount of catalyst (continuously renewed by diffusion), these results strongly suggest that functionalization of the electrode surface greatly enhances the catalyst stability during CO<sub>2</sub> electrochemical reduction.

Insert Figure 6 and 7 HERE

#### GC measurements.

We collected Gas Chromatographic data with the aim to evaluate the amount of CO and H<sub>2</sub> produced during exhaustive electrolysis. Our experimental setup consists in applying a potential of -2.10 V vs. Fc/Fc+ with a CO<sub>2</sub> constant flow of 40

Insert Figure 8

ml/min, and sampling the gas in the electrochemical cell at regular interval times (see experimental section). At non-modified GCE and in homogeneous solutions, complexes **1**, **2** and **3** show different degree of selectivity towards CO with a CO/H<sub>2</sub> ratio of 44, 11 and 8, respectively. The faradic efficiencies  $\eta_{\text{CO}}$  are 97.5%, 35.4% and 46.4%, while TON<sub>CO</sub> after 60 min are 3.8, 1.7 and 3.9 for the complexes **1**, **2** and **3**, respectively (Table 4). These values are worse than the Lehn's catalyst (bpy)Re(CO)<sub>3</sub>Cl in the same conditions.<sup>14</sup> Another unexpected feature of the homogeneous solution is that all the catalysts apparently suffer of rapid deactivation in relative short time.

However, if after 60 min the GCE is sonicated, the catalytic current is reactivated. Moreover, compounds **2** and **3** have a low  $\eta_{\text{CO}}$ . We suppose that the products of CO<sub>2</sub> reduction and thiophene units, especially for **2** and **3**, might interact with GCE and undergo in long time scale physical adsorption, altering the nature of the catalytic specie. The absorption on the surface of these reaction products probably reduce  $\eta_{\text{CO}}$  and the apparent catalyst lifetimes. The variation of  $\eta_{\text{CO}}$  during the exhaustive electrolysis is particular evident for complex **3** (see Fig. S7). We cannot exclude, also, that chemical reactions with CO<sub>2</sub> occur at thiophene moiety, or at the C≡C triple bond of **3** where the contributions of sp carbon atoms to the LUMO appear to be relevant (Fig. S4).

On the other hand, TON<sub>CO</sub> of the electrodes modified with **2** and **3** show significant improvements (Table 4). Surprisingly, GCE modified with **2** has a much higher  $\eta_{\text{CO}}$  (84.7%) than its homogeneous solution counterpart (35.4%), whereas  $\eta_{\text{CO}}$  of **3** is almost unvaried. It is interesting to note that both electrodes modified with monomer containing C≡C triple bond, 5,5'-bis-(phenylethynyl)-2,2'-bipyridine and **3**, shows low similar  $\eta_{\text{CO}}$  values. It should be mentioned that in only 10 minutes of the catalytic activity of our surface-modified GCE with **2** and **3**, the overall TON<sub>CO</sub> of 201 and 288 are already achieved, respectively. The final TON<sub>CO</sub> of 489 and 519 of complexes **2** and **3** for 40 min, are among the best values reported in the literature for analogues surface-modified electrodes.

## Conclusions

We reported novel bipyridine ligands carrying thiophene (**T**), 2,2':5',2''-terthiophene (**TT**) and 3'-ethynyl 2,2':5',2''-terthiophene (**ETT**), and synthesized their corresponding tricarbonyl chlororhenium complexes. Their electrochemical oxidation on GCE allows depositing stable electron conducting films that carry rhenium complexes. These chemical modified electrodes were used to investigate the electrocatalytic reduction of CO<sub>2</sub>. This approach may represent an alternative pathway to support the desired intact organometallic catalyst on an electrode surface.

A relative comparison outlines that activity and lifetime of the solid-supported catalysts are greatly enhanced with respect the corresponding homogeneous counterparts. A rough estimation of the TOFs (both in homogeneous and in heterogeneous phase) and their lifetimes can be obtained by CVs and repeated CV scans or by chronoamperometric measurements, respectively. Electro-polymerized (**TT**)Re(CO)<sub>3</sub>Cl (**2**) and (ETT)Re(CO)<sub>3</sub>Cl (**3**) show a relative higher stability towards their reduction than the corresponding homogeneous solutions, similarly as observed for a vinylterpyridinyl complex of cobalt.<sup>58</sup> This suggests that the proximity with the surface may protect the active form of the catalysts against its decomposition, which is higher in homogeneous solution. The film of **3** is slightly less stable than that of **2**, while their catalytic activities are almost equivalent. A change of selectivity is observed for **3**, apparently due to the C≡C triple bond. Thus, this observation may suggests that either the reduced ethynyl group reacts with CO<sub>2</sub> and/or pushes the rhenium center of the electro-polymerized **3** towards the solution, making it more exposed to the effects of the solution. Unfortunately our attempts to use the OTTE spectroelectrochemical cell to investigate the deactivation process did not resulted in any useful data, probably because Pt-S interactions on the Pt minigrad electrode.

Larger film thickness gave higher catalytic current, but lower  $i_c/i_p$  ratio, suggesting that only the rhenium metal centres on the top of the electrodeposited polymer surface are catalytically active. Although no final conclusions can be extrapolated from the data reported in Table 4, it seems that the insertion of functional groups like CO<sub>2</sub> or C≡C decreases the selectivity of CO<sub>2</sub> reduction to CO, probably because increased local electron density and hence localized reactivity towards the weak electrophile CO<sub>2</sub>. This observation should be taken in account for the design of new generation of electrode-modified catalysts, where the electron conduction properties of the employed polymers appear to be somewhat beneficial, but it should be carefully selected. Finally, the applied potential for the reduction of CO<sub>2</sub> to CO for **2** and **3** in acetonitrile is comparable with other monomers reported in Table 4 (between -1.9 and -2.2 V vs. Fc<sup>0/+</sup>), being those typical of Re(bpy)-type complexes.

## Experimental Section

### Materials and Reagents

Reagents were purchased from Alfa Aesar and Aldrich and used without further purification. Acetonitrile was distilled over calcium hydride just before use. All reactions were performed under inert atmosphere. Microwave

(MW) reactions were carried out in single-mode Biotage Initiator 2.5. Column chromatography was done on a Biotage Isolera flash purification system. Mass spectra were recorded with an XCT PLUS electrospray ionization ion trap (ESIIT) mass spectrometer (Agilent Italy, Milan). Samples were dissolved in methanol. The samples for microanalyses were dried under vacuum to constant weight (25 °C, ca. 0.1 torr). Elemental analyses (C, H, N, S) were performed in-house with a Fisons 1108 CHNS-O elemental analyzer. Infrared spectra were recorded as powder ATR with a Bruker Equinox 55 FTIR spectrophotometer with a resolution of 1 cm<sup>-1</sup> and an accumulation of 64 scans. NMR spectra were recorded with a Bruker Avance 200 and a JEOL EX 400 spectrometer (1H operating frequency 400 MHz) at 298 K. <sup>1</sup>H chemical shifts are relative to TMS ( $\delta = 0$  ppm) and referenced against solvent residual peaks. Electrochemical experiments were carried out in freshly distilled acetonitrile with TBAPF<sub>6</sub> 0.1 M as supporting electrolyte, in the usual conditions employing an Autolab PGSTAT302N electrochemical analyzer controlled by a PC. A pure silver wire was used as pseudo reference, platinum wire as counter electrode and Glassy Carbon Electrode (GCE) as working electrode. Under our experimental conditions, all the potentials are shown versus the half-wave potential of the ferrocene redox couple (Fc/Fc<sup>+</sup>). The ferrocene diffusion coefficient has been taken from the literature:  $D_{Fc} = 2.24 \times 10^{-5}$  cm<sup>2</sup>/s.<sup>66, 67</sup>

### Computational Details

All calculations were performed using Gaussian 09 Rev. D.01<sup>68</sup> adopting the DFT method, including the solvent effect by the conductor-like polarizable continuum model (CPCM)<sup>69, 70</sup> with acetonitrile as solvent. Geometry optimizations were carried out without any constraints by using the B3LYP functional<sup>71, 72</sup> employing the optimized def2SVPP basis set<sup>73, 74</sup> with the D3 version of Grimme's dispersion and applying the Becke-Johnson damping scheme.<sup>75</sup> Thermal correction to Gibbs Free Energy has been applied with a scale factor of 0.962 to the IR frequency to take in account the anisotropy. For radical anions, unrestricted Kohn–Sham formalism (UKS) was adopted. The nature of all stationary points were confirmed by normal-mode analysis (no imaginary frequencies were found). DFT calculation of redox potentials were performed applying the literature method<sup>51, 52, 76</sup> that consists into computing the Gibbs free energy in solution of both the oxidized and reduced species with respect that of the reference compound ferrocene.

### Syntheses

More details and scheme of the syntheses of the organic ligands **T**, **TT** and **ETT** are reported in the ESI material.

**4-(thiophen-3-yl)-2,2'-bipyridine (T)**: To 20 ml of DME, previously purged with argon, 4-Bromo-2,2'-bipyridine (0.5 g, 2.13 mmol) and Pd(PPh<sub>3</sub>)<sub>4</sub> (0.246 g, 0.213 mmol, 0.1 eq) were added and further purged with argon for 10 min. Boronic acid (0.299 g, 0.234 mmol, 1.1 eq) was added and purged for 5 min, after which a Na<sub>2</sub>CO<sub>3</sub> solution (2 M, 8.51 mmol, 4 eq) was added and purged for 10 min. The mixture was reacted under MW irradiation for 30 min, filtered to remove the solid and evaporated under reduced pressure. Water was added (10 ml) and the crude product mixture was extracted with diethyl ether (3×10 ml). The organic phase was dried over Na<sub>2</sub>SO<sub>4</sub>, filtered and evaporated under reduced pressure. The product was purified by medium pressure flash chromatography (Biotage) on a 50 g column, with petroleum ether: ethyl acetate 80:20 + 0.05% triethylamine (TEA) as additive. Yield: 80%. <sup>1</sup>H NMR (400 MHz, ppm, acetone-d<sub>6</sub>):  $\delta$  8.77 (dd, J=1.8, 0.6 Hz, 1H), 8.71 (dq, J=4.7, 0.9 Hz, 1H), 8.68 (dd, J=5.0, 0.6 Hz, 1H), 8.51 (dt, J=8.2, 1.0 Hz, 1H), 8.16 (dd, J=2.9, 1.5 Hz, 1H), 7.94 (td, J=7.9, 1.8 Hz, 1H), 7.75-7.72 (m, 2H), 7.70-7.68 (m, 1H), 7.42-7.45 (m, 1H). LC-MS (ESI<sup>+</sup>) calcd. for C<sub>14</sub>H<sub>10</sub>N<sub>2</sub>S [M+H<sup>+</sup>] 239.06, found 239.25.

**[2,2':5',2''-terthiophen]-3'-ylboronic acid (TTB, 7)**, see ESI). In a Schlenk 20 mL round bottom flask, a solution of 3'-bromoterthiophene (0.668 g, 2.04 mmol) and trimethyl borate (0.276 g, 0.296 mL, 2.65 mmol), in 8 ml THF was treated with n-BuLi (1.6M in hexanes, 1.658 ml, 2.65 mmol) at -78°C over a period of 20 minutes. The resulting solution was stirred at -78°C for an hour. The solution was then warmed up to -20°C in 1h, quenched slowly using 2N HCl (1.326 mL, 2.65 mmol) and then stirred for 4 h. 2,2':5',2''-terthiophen-3'-ylboronic acid (**TTB**, **7**) was precipitated out as a white solid, washed with water and dried under reduced pressure. The crude **TTB** was directly used for the next step.

**4-([2,2':5',2''-terthiophen]-3'-yl)-2,2'-bipyridine (TT)**. To a degassed solution of 4-bromo-2,2'-bipyridine (0.1013 g, 0.431 mmol, 0.9 eq) and Pd(PPh<sub>3</sub>)<sub>4</sub> (55 mg, 0.048 mmol, 0.1 eq.) in dimethoxyethane (DME, 5 mL) 7 mL of a solution of **TTB (7)** (0.140 g, 0.479 mmol, 1 eq) in dimethoxyethane was added. Finally, 0.480 ml of a 2M solution of Na<sub>2</sub>CO<sub>3</sub> (0.102 g, 0.962 mmol, 2 eq.) in water was added. The reaction mixture was heated at 120 °C for 30 min under MW irradiation. The reaction was controlled by TLC (dichloromethane: ethyl acetate 4:6 + TEA 0.1%) (R<sub>f</sub> = 0,26). When the starting material was fully consumed, the solvent was removed at low pressure. Water (5 mL) was added and the product was extracted with ethyl acetate (5×5 mL). The organic phases were collected, dried over Na<sub>2</sub>SO<sub>4</sub>, and filtered. The crude reaction product (0.4964 g) was purified by medium pressure flash chromatography (Biotage) on a 50 g column, with dichloromethane: ethyl acetate 70:30 + 0,5 % TEA as additive. Yield: 43%. <sup>1</sup>H NMR (200 MHz, CDCl<sub>3</sub>, ppm)  $\delta$  8.65 (d, J = 4.4 Hz, 1H), 8.57 (d, J = 5.0 Hz, 1H), 8.47 (d, J = 0.9 Hz,



1H), 8.39 (d, J = 8.0 Hz, 1H), 7.80 (td, J = 7.9, 1.8 Hz, 1H), 7.38 – 7.12 (m, 6H), 7.08 – 6.97 (m, 2H), 6.93 (dd, J = 5.0, 3.6 Hz, 1H). LC-MS (ESI<sup>+</sup>) calcd. for C<sub>22</sub>H<sub>14</sub>N<sub>2</sub>S<sub>3</sub> [M+H<sup>+</sup>] 403.03, found 403.28.

**4-[(2,2':5',2''-terthiophen)-3'-ylethynyl]-2,2'-bipyridine (ETT)**. In a 100 mL round bottom flask equipped with a condenser, a magnetic stirrer and Ar inlet, 4-bromo-2,2'-bipyridine (0.302 g, 1.285 mmol), Pd(PPh<sub>3</sub>)<sub>4</sub> (0.074 g, 0.064 mmol), CuI (0.024 g, 0.1284 mmol), 3'-ethynyl-2,2':5',2''-terthiophene (0.350 g, 1.285 mmol) (**6**, see ESI) were added and dissolved with 1,4-dioxane/H<sub>2</sub>O 3:1 (32 mL). Finally triethylamine (0.260 g, 2.57 mmol) was added. The reaction mixture was then refluxed under Ar for 17-22h and checked by TLC (petroleum ether:ethyl acetate 7:3 + TEA 0,1%) to monitor the disappearance of 3'-ethynyl-2,2':5',2''-terthiophene. After cooling to RT, the mixture was filtered off, the 1,4-dioxane evaporated under reduced pressure. Water was added (40 mL) and the solution was washed with dichloromethane (3×20 ml). The combined organic phase was dried over Na<sub>2</sub>SO<sub>4</sub>, and evaporated to dryness under reduced pressure. The residue was purified by medium pressure flash chromatography (Biotage) with a 50 g column, using petroleum ether:ethyl acetate (8:2) as eluant and 0.1% TEA as additive. **ETT** was obtained as a yellow oil. Yield: 30%. <sup>1</sup>H NMR (400 MHz, ppm, acetone-d<sub>6</sub>): δ 8.92 (s, 1H), 8.83-8.85 (m, 2H), 8.75 (d, J=7.6 Hz, 1H), 8.26-8.29 (m, 1H), 8.76-8.77 (m, 2H), 7.68-7.69 (m, 2H), 7.54 (d, J=5.1 Hz, 1H), δ=7.45 (s, 1H), 7.43 (dd, J=3.5, 0.9 Hz, 1H), 7.23 (dd, J=5.0, 3.8 Hz, 1H), 7.15 (dd, J=5.4, 3.5 Hz, 1H). LC-MS (ESI<sup>+</sup>) calcd. for C<sub>24</sub>H<sub>14</sub>N<sub>2</sub>S<sub>3</sub> [M+H<sup>+</sup>] 427.03, found 427.11.

The synthesis of complexes **1**, **2** and **3** proceed in a similar way as previously reported.<sup>13,15</sup> Chloropentacarbonylrhenium(I) Re(CO)<sub>5</sub>Cl (0.130 g, 0.36 mmol) and **T** (0.088 g, 0.37 mmol) for **1** (0.148 g **TT** for **2**, 0.158 g **TTE** for **3**) were dissolved in toluene. The solution was degassed and heated to reflux under Ar for 2 h. The precipitate was collected by centrifugation, and washed with 3×5ml of petroleum ether and 3×5ml of dichloromethane. Yellow solids were obtained after drying under vacuum, with an overall yields around 70-76%.

(**T**)Re(CO)<sub>3</sub>Cl (**1**): <sup>1</sup>H NMR (400 MHz, ppm, acetone-d<sub>6</sub>): ): 9.12 (d, J=5.6 Hz, 1H), δ=9.04 (d, J=5.9 Hz, 1H), 8.99 (s, 1H), 8.9 (d, J=9.1 Hz, 1H), 8.48 (dd, J=3.0, 1.5 Hz, 1H), 8.36 (t, 1H, J=7.6 Hz, 1H), 8.07 (d, J=5.9 Hz, 1H), 7.93 (dd, J=5.3, 1.4 Hz, 1H) 7.76-7.82 (m, 2H). ν<sub>CO</sub> IR (MeCN): 2023, 1917, 1901 cm<sup>-1</sup>; ATR-IR: 2011, 1918, 1886, 1852 cm<sup>-1</sup>. C<sub>17</sub>H<sub>11</sub>ClN<sub>2</sub>O<sub>3</sub>ReS (545.01); calcd.: C 37.46, H 2.03, N 5.14, S 5.88; found: C 37.37, H 1.99, N 5.10, S 5.83.

(**TT**)Re(CO)<sub>3</sub>Cl (**2**): <sup>1</sup>H NMR (400 MHz, ppm, acetone-d<sub>6</sub>): ): 9.13 (d, J=5.0 Hz, 1H), 9.03 (d, J=7.2 Hz, 1H), 8.76 (s, 1H), 8.64 (d, J=8.2 Hz, 1H), 8.33 (td, J=7.9, 1.4 Hz, 1H), 7.96 (s, 1H), 7.81 (t, J=6.5 Hz, 1H), 7.72-7.74 (m, 2H) 7.62 (dd, J=5.0, 0.9 Hz, 1H), 7.55 (d, 1H, J=5.4 Hz, 1H), 7.44 (d, 1H, J=3.7 Hz, 1H), 7.26 (d, 1H, J=4.1 Hz, 1H), 7.55 (d, J=5.4 Hz, 1H), 7.15-7.17 (m, 1H). ν<sub>CO</sub> IR (MeCN): 2024, 1918, 1902 cm<sup>-1</sup>; ATR-IR: 2018, 1905, 1879, 1864 cm<sup>-1</sup>. C<sub>25</sub>H<sub>15</sub>ClN<sub>2</sub>O<sub>3</sub>ReS<sub>3</sub> (709.25): calcd.: C 42.34, H 2.13, N 3.95, S, 13.56; found: C 42.01, H 2.08, N 3.89, S 13.50.

(**TTE**)Re(CO)<sub>3</sub>Cl (**3**): <sup>1</sup>H NMR (400 MHz, ppm, acetone-d<sub>6</sub>): ): 9.12-9.15(m, 2H), 8.80-8.82 (m, 2H), 8.38 (t, J=7.9 Hz, 1H), 7.91 (d, J=5.7 Hz, 1H), 7.83 (t, J=6.5 Hz, 1H), 7.66-7.70 (m, 2H), 7.56 (d, J=7.5 Hz, 1H), 7.43 (dd, J=3.5, 1.2 Hz, 1H), 7.41 (s, 1H), 7.20-7.23 (m, 1H), 7.14-7.17 (m, 1H). ν<sub>CO</sub> IR (MeCN): 2023, 1919, 1904 cm<sup>-1</sup>; ATR-IR: 2017, 1913, 1879, 1866 cm<sup>-1</sup>. C<sub>27</sub>H<sub>15</sub>ClN<sub>2</sub>O<sub>3</sub>ReS<sub>3</sub> (733.27) calcd.: C 44.22, H 2.06, N 3.82, S, 13.12; found: C 44.05, H 2.00, N 3.78, S 13.02.

## GC Measurements

The airtight electrochemical cell was equipped with a bubbler that maintained the inner atmosphere<sup>15</sup> but avoided gas overpressure. A Smart Trak 100 (Sierra) mass flow controller C100L was used to measure and control the CO<sub>2</sub> flow during exhaustive electrolysis experiments. A constant CO<sub>2</sub> flow (40 mL min<sup>-1</sup>) was maintained during bulk electrolysis. To ensure high surface area and fast electrochemical conversion, a cylindrical rod (ø = 5 mm, length 15 mm) of large surface area (2.55 cm<sup>2</sup>) was used as GCE. Bulk electrolysis of complex **1**, **2** and **3** (4.6, 1.9 and 1.0 μmol in 5 ml of acetonitrile, respectively) were dissolved in as many solutions for catalytic tests. The same GCE was carefully polished and cleaned every experiments with alumina nanopowder, functionalized by 5 CV oxidative cycles starting from the solution of complex **2** and **3**, resulting in 21×10<sup>-10</sup> and 11×10<sup>-10</sup> mol (evaluated by charge integration of CVs), respectively. The gas sample produced was analyzed with an Agilent 490 Micro GC gas chromatograph equipped with a Molsieve column (5 Å) and a CP-PoraPLOT U column. A thermal conductivity detector was used for CO and H<sub>2</sub> quantification and the Molsieve column (5 Å) was kept at a temperature of 90 °C and at a pressure of 200 kPa. The carrier gas was argon. The gas inside the measurement cell was sampled for 90 s to wash and fill the Micro GC 10 μL sample loop, and eventually 500 nL were injected into each column for the analyses. It was possible to determine the amounts of CO and H<sub>2</sub> produced during the experiment from the concentrations of CO and H<sub>2</sub> in the gas samples and knowledge of the gas flow and the cell volume. For the functioning and the calibration of the GC apparatus, Ar, He, N<sub>2</sub>, O<sub>2</sub>, CO<sub>2</sub> and CO were obtained from Sapio, whereas H<sub>2</sub> was produced by a ClaindHyGen hydrogen generator. The detection limits for CO and H<sub>2</sub> were 20 and 0.5 ppm (v/v), respectively.

## Acknowledgements

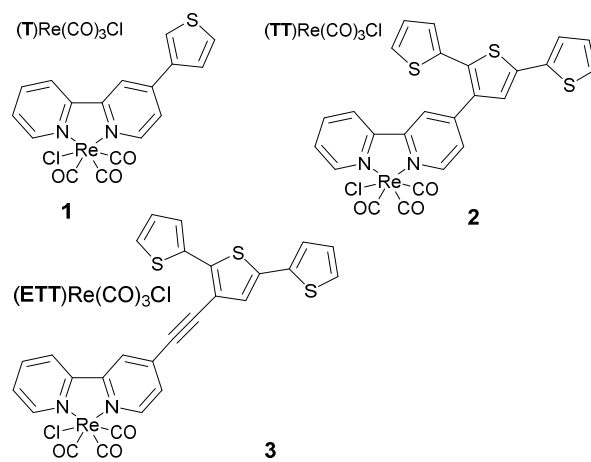
Financial supports from China Scholarship Council (CSC), the Compagnia di San Paolo and Università di Torino (PHOTORECARB project) are gratefully acknowledged. We also thank Dr. Fabrizio Sordello and Federico Franco (University of Turin) for helps in GC measurements.

## Notes and references

1. J. M. Savéant, *Chem. Rev.*, 2008, **108**, 2348-2378.
2. E. E. Benson, C. P. Kubiak, A. J. Sathrum and J. M. Smieja, *Chem. Soc. Rev.*, 2009, **38**, 89-99.
3. M. L. Clark, K. A. Grice, C. E. Moore, A. L. Rheingold and C. P. Kubiak, *Chem. Sci.*, 2014, **5**, 1894-1900.
4. C. Costentin, S. Drouet, M. Robert and J. M. Savéant, *Science*, 2012, **338**, 90-94.
5. J. Ronge, T. Bosserez, D. Martel, C. Nervi, L. Boarino, F. Taulelle, G. Decher, S. Bordiga and J. A. Martens, *Chem. Soc. Rev.*, 2014, **43**, 7963-7981.
6. M. G. Mali, H. Yoon, B. N. Joshi, H. Park, S. S. Al-Deyab, D. C. Lim, S. Ahn, C. Nervi and S. S. Yoon, *ACS Appl. Mater. Interfaces*, 2015, **7**, 21619-21625.
7. E. Fujita, D. J. Szalda, C. Creutz and N. Sutin, *J. Am. Chem. Soc.*, 1988, **110**, 4870-4871.
8. E. Fujita, C. Creutz, N. Sutin and D. J. Szalda, *J. Am. Chem. Soc.*, 1991, **113**, 343-353.
9. J. Grodkowski, P. Neta, E. Fujita, A. Mahammed, L. Simkhovich and Z. Gross, *J. Phys. Chem. A*, 2002, **106**, 4772-4778.
10. E. Simon-Manso and C. P. Kubiak, *Organometallics*, 2005, **24**, 96-102.
11. J. W. Raebiger, J. W. Turner, B. C. Noll, C. J. Curtis, A. Miedaner, B. Cox and D. L. DuBois, *Organometallics*, 2006, **25**, 3345-3351.
12. C. Costentin, G. Passard, M. Robert and J. M. Savéant, *J. Am. Chem. Soc.*, 2014, **136**, 11821-11829.
13. F. Franco, C. Cometto, F. F. Vallana, F. Sordello, E. Priola, C. Minero, C. Nervi and R. Gobetto, *Chem. Commun.*, 2014, **50**, 14670-14673.
14. F. Franco, C. Cometto, C. Garino, C. Minero, F. Sordello, C. Nervi and R. Gobetto, *Eur. J. Inorg. Chem.*, 2015, 296-304.
15. F. Franco, C. Cometto, C. Minero, L. Nencini, J. Fiedler, R. Gobetto and C. Nervi, *ChemElectroChem*, 2015, **2**, 1372-1379.
16. J. Hawecker, J. M. Lehn and R. Ziessel, *J. Chem. Soc. Chem. Commun.*, 1984, DOI: 10.1039/C39840000328, 328-330.
17. J. M. Smieja and C. P. Kubiak, *Inorg. Chem.*, 2010, **49**, 9283-9289.
18. J. D. Blakemore, A. Gupta, J. J. Warren, B. S. Brunschwig and H. B. Gray, *J. Am. Chem. Soc.*, 2013, **135**, 18288-18291.
19. C. Riplinger, M. D. Sampson, A. M. Ritzmann, C. P. Kubiak and E. A. Carter, *J. Am. Chem. Soc.*, 2014, **136**, 16285-16298.
20. S. A. Chabolla, E. A. Dellamary, C. W. Machan, F. A. Tezcan and C. P. Kubiak, *Inorg. Chim. Acta*, 2014, **422**, 109-113.
21. J. J. Teesdale, A. J. Pistner, G. P. A. Yap, Y. Z. Ma, D. A. Lutterman and J. Rosenthal, *Cat. Today*, 2014, **225**, 149-157.
22. C. W. Machan, S. A. Chabolla, J. Yin, M. K. Gilson, F. A. Tezcan and C. P. Kubiak, *J. Am. Chem. Soc.*, 2014, **136**, 14598-14607.
23. K. A. Grice and C. P. Kubiak, in *CO<sub>2</sub> Chemistry*, eds. M. Aresta and R. V. Eldik, 2014, vol. 66, pp. 163-188.
24. K. J. Young, L. A. Martini, R. L. Milot, R. C. Snoeberger, III, V. S. Batista, C. A. Schmuttenmaer, R. H. Crabtree and G. W. Brudvig, *Coord. Chem. Rev.*, 2012, **256**, 2503-2520.
25. T. R. Otoole, L. D. Margerum, T. D. Westmoreland, W. J. Vining, R. W. Murray and T. J. Meyer, *J. Chem. Soc. Chem. Commun.*, 1985, 1416-1417.
26. T. R. Otoole, B. P. Sullivan, M. R. M. Bruce, L. D. Margerum, R. W. Murray and T. J. Meyer, *J. Electroanal. Chem.*, 1989, **259**, 217-239.
27. K. C. Cheung, P. Guo, M. H. So, L. Y. S. Lee, K. P. Ho, W. L. Wong, K. H. Lee, W. T. Wong, Z. Y. Zhou and K. Y. Wong, *J. Organomet. Chem.*, 2009, **694**, 2842-2845.
28. E. Portenkirchner, K. Oppelt, C. Ulbricht, D. A. M. Egbe, H. Neugebauer, G. Knoer and N. S. Sariciftci, *J. Organomet. Chem.*, 2012, **716**, 19-25.
29. E. Portenkirchner, J. Gasiorowski, K. Oppelt, S. Schlager, C. Schwarzinger, H. Neugebauer, G. Knoer and N. S. Sariciftci, *ChemCatChem*, 2013, **5**, 1790-1796.
30. F. Cecchet, M. Alebbi, C. A. Bignozzi and F. Paolucci, *Inorg. Chim. Acta*, 2006, **359**, 3871-3874.
31. C. R. Cabrera and H. D. Abruna, *J. Electroanal. Chem.*, 1986, **209**, 101-107.
32. S. Cosnier, A. Deronzier and J. C. Moutet, *J. Electroanal. Chem.*, 1986, **207**, 315-321.
33. S. Cosnier, A. Deronzier and J. C. Moutet, *J. Mol. Cat.*, 1988, **45**, 381-391.
34. T. Yoshida, K. Tsutsumida, S. Teratani, K. Yasufuku and M. Kaneko, *J. Chem. Soc. Chem. Commun.*, 1993, 631-633.
35. M. Sandroni, G. Volpi, J. Fiedler, R. Buscaino, G. Viscardi, L. Milone, R. Gobetto and C. Nervi, *Cat. Today*, 2010, **158**, 22-28.

36. N. D. Schley, J. D. Blakemore, N. K. Subbaiyan, C. D. Incarvito, F. D'Souza, R. H. Crabtree and G. W. Brudvig, *J. Am. Chem. Soc.*, 2011, **133**, 10473-10481.
37. A. Krawicz, J. Yang, E. Anzenberg, J. Yano, I. D. Sharp and G. F. Moore, *J. Am. Chem. Soc.*, 2013, **135**, 11861-11868.
38. C. Costentin, S. Drouet, M. Robert and J. M. Savéant, *J. Am. Chem. Soc.*, 2012, **134**, 11235-11242.
39. C. Costentin, S. Drouet, M. Robert and J. M. Savéant, *J. Am. Chem. Soc.*, 2012, **134**, 19949-19950.
40. M. Delamar, R. Hitmi, J. Pinson and J. M. Savéant, *J. Am. Chem. Soc.*, 1992, **114**, 5883-5884.
41. M. O. Wolf, *Advanced Materials*, 2001, **13**, 545-553.
42. H. Siringhaus, N. Tessler and R. H. Friend, *Science*, 1998, **280**, 1741-1744.
43. M. R. Andersson, O. Thomas, W. Mammo, M. Svensson, M. Theander and O. Inganäs, *J. Mat. Chem.*, 1999, **9**, 1933-1940.
44. D. T. McQuade, A. E. Pullen and T. M. Swager, *Chem. Rev.*, 2000, **100**, 2537-2574.
45. G. Li, V. Shrotriya, J. S. Huang, Y. Yao, T. Moriarty, K. Emery and Y. Yang, *Nature Mater.*, 2005, **4**, 864-868.
46. J. H. Yoon, D. M. Kim, S. S. Yoon, M. S. Won and Y. B. Shim, *J. Power Sources*, 2011, **196**, 8874-8880.
47. D. M. Kim, J. H. Yoon, M. S. Won and Y. B. Shim, *Electrochim. Acta*, 2012, **67**, 201-207.
48. F. P. A. Johnson, M. W. George, F. Hartl and J. J. Turner, *Organometallics*, 1996, **15**, 3374-3387.
49. B. P. Sullivan, C. M. Bolinger, D. Conrad, W. J. Vining and T. J. Meyer, *J. Chem. Soc. Chem. Commun.*, 1985, DOI: Article, 1414-1415.
50. L. Groenendaal, G. Zotti and F. Jonas, *Synth. Met.*, 2001, **118**, 105-109.
51. P. Zanello, C. Nervi and F. Fabrizi De Biani, *Inorganic Electrochemistry. Theory, Practice and Application*, RSC, Cambridge, 2<sup>nd</sup> edn., 2011.
52. L. E. Roy, E. Jakubikova, M. G. Guthrie and E. R. Batista, *J. Phys. Chem. A*, 2009, **113**, 6745-6750.
53. A. Gennaro, A. A. Isse and E. Vianello, *J. Electroanal. Chem.*, 1990, **289**, 203-215.
54. D. L. DuBois, A. Miedaner and R. C. Haltiwanger, *J. Am. Chem. Soc.*, 1991, **113**, 8753-8764.
55. B. P. Sullivan, M. R. M. Bruce, T. R. Otoole, C. M. Bolinger, E. Megehee, H. Thorp and T. J. Meyer, *ACS Symp. Ser.*, 1988, **363**, 52-90.
56. K. Takada, G. D. Storrer, F. Pariente and H. D. Abruna, *J. Phys. Chem. B*, 1998, **102**, 1387-1396.
57. B. B. Cui, H. J. Nie, C. J. Yao, J. Y. Shao, S. H. Wu and Y. W. Zhong, *Dalton Trans.*, 2013, **42**, 14125-14133.
58. A. R. Guadalupe, D. A. Usifer, K. T. Potts, H. C. Hurrell, A. E. Mogstad and H. D. Abruna, *J. Am. Chem. Soc.*, 1988, **110**, 3462-3466.
59. H. Dahms, *J. Phys. Chem.*, 1968, **72**, 362-364.
60. I. Ruff, *Electrochim. Acta*, 1970, **15**, 1059-1061.
61. I. Ruff and I. Korosi-Odor, *Inorg. Chem.*, 1970, **9**, 186-188.
62. I. Ruff and V. J. Friedrich, *J. Phys. Chem.*, 1971, **75**, 3297-3302.
63. A. J. Bard and L. R. Faulkner, *Electrochemical Methods*, Wiley, New York, 2<sup>nd</sup> Edition edn., 2001.
64. B. Barbier, J. Pinson, G. Desarmot and M. Sanchez, *J. Electrochem. Soc.*, 1990, **137**, 1757-1764.
65. D. Osella, L. Milone, C. Nervi and M. Ravera, *J. Organomet. Chem.*, 1995, **488**, 1-7.
66. K. M. Kadish, J. Q. Ding and T. Malinski, *Anal. Chem.*, 1984, **56**, 1741-1744.
67. N. G. Tsierkezos, *J. Solution Chem.*, 2007, **36**, 289-302.
68. M. J. Frisch et al. Gaussian 09, Revision. D.01, Gaussian, Inc., Wallingford CT, 2009.
69. S. Miertuš, E. Scrocco and J. Tomasi, *Chem. Phys.*, 1981, **55**, 117-129.
70. M. Cossi, G. Scalmani, N. Rega and V. Barone, *J. Chem. Phys.*, 2002, **117**, 43-54.
71. A. D. Becke, *J. Chem. Phys.*, 1993, **98**, 5648-5652.
72. C. Lee, W. Yang and R. G. Parr, *Phys. Rev. B: Condens. Matter*, 1988, **37**, 785-789.
73. F. Weigend and R. Ahlrichs, *Phys. Chem. Chem. Phys.*, 2005, **7**, 3297-3305.
74. F. Weigend, *Phys. Chem. Chem. Phys.*, 2006, **8**, 1057-1065.
75. S. Grimme, S. Ehrlich and L. Goerigk, *J. Comput. Chem.*, 2011, **32**, 1456-1465.
76. D. H. Evans, *Chem. Rev.*, 2008, **108**, 2113-2144.

## Schemes



Scheme 1. The synthesized ligands and complexes.

# Figures

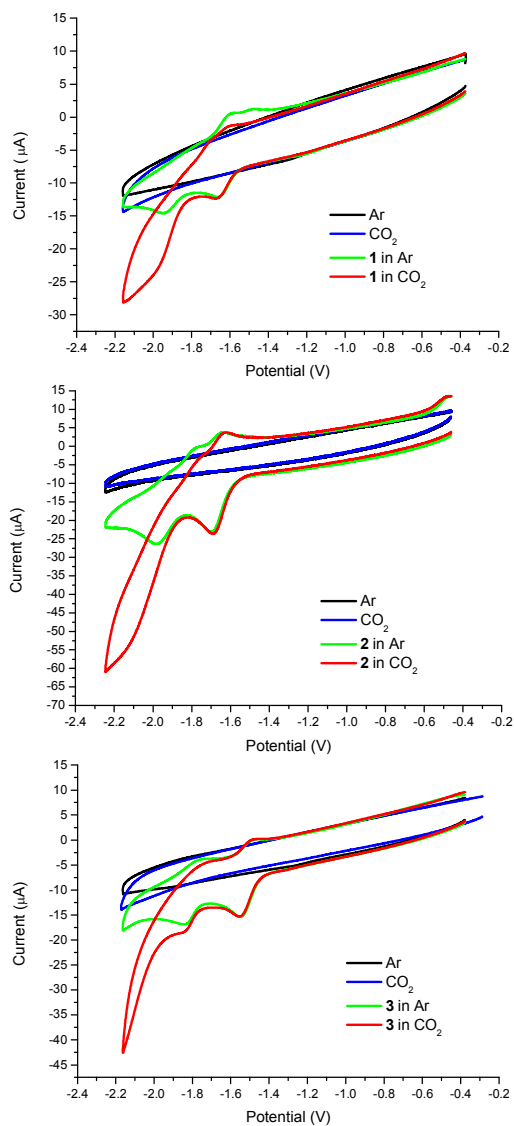
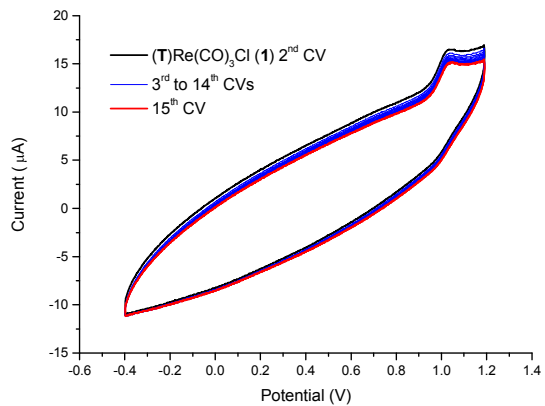


Figure 1. CV of complexes **1**, **2** and **3** in MeCN



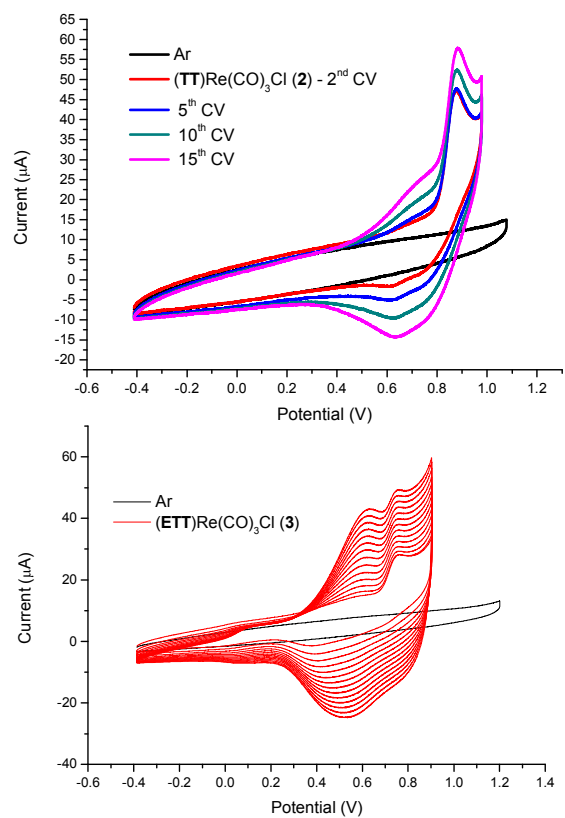


Figure 2. Oxidation CV cycles, at 0.2 V/s for the modification of electrode for complex **1**, **2** and **3**.

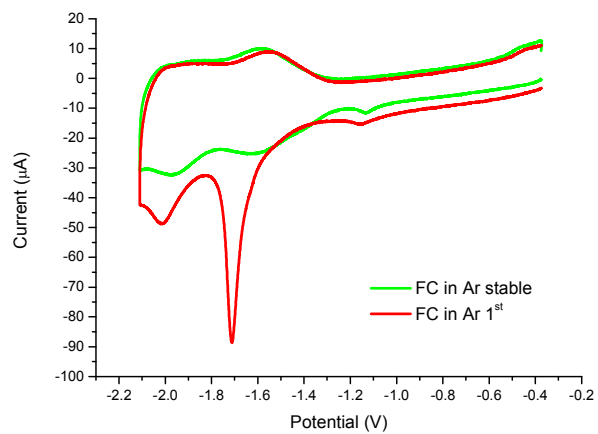


Figure 3. First and steady state CVs of the electrode modified with complex **2** at scan rate 0.2 V/s, with  $\Gamma = 7.74 \times 10^{-10}$  mol/cm<sup>2</sup>.

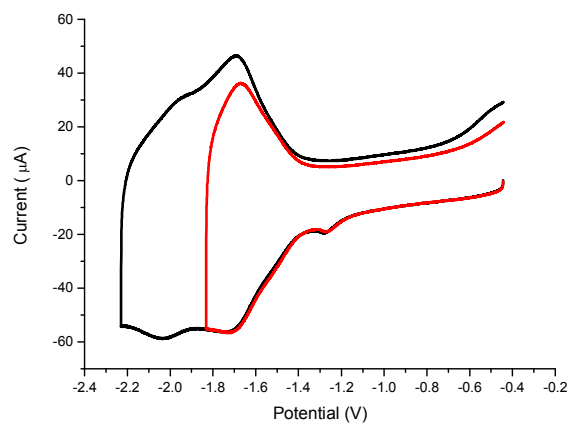


Figure 4. CVs (scan rate 2.0 V/s) of the steady-state electrode modified by complex **2**, with  $\Gamma = 7.74 \times 10^{-10} \text{ mol/cm}^2$ .

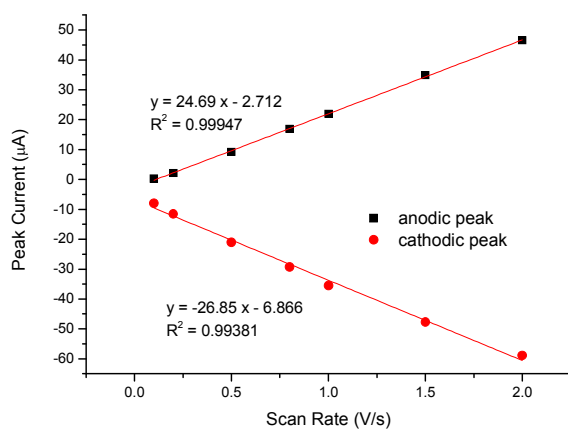


Figure 5. Electrode modified with complex **2** with coverage  $7.74 \times 10^{-10} \text{ mol/cm}^2$ .

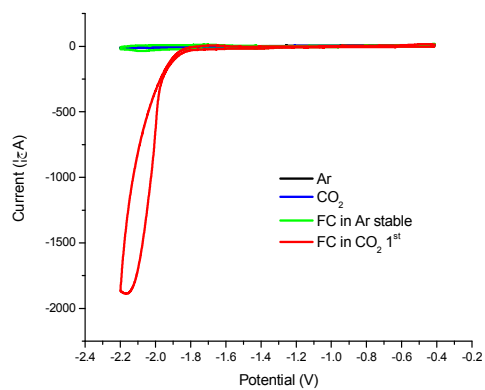


Figure 6. First reduction CV cycle of the functional electrode modified by complex **2** at scan rate 0.2 V/s, with  $\Gamma = 35.30 \times 10^{-10} \text{ mol/cm}^2$

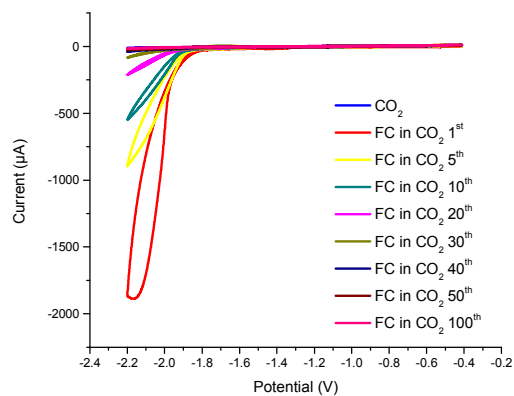


Figure 7. CV cycles of the electrode modified by complex **2** at scan rate 0.2 V/s, with  $\Gamma = 35.30 \times 10^{-10}$  mol/cm<sup>2</sup>.

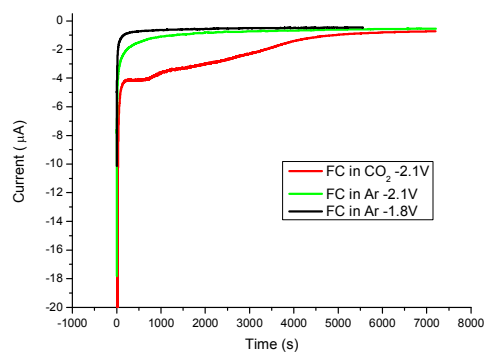


Figure 8. Chronoamperometry of electrode functionalized by complex **2** under Ar and CO<sub>2</sub>, with  $\Gamma = 9.55 \times 10^{-10}$  mol/cm<sup>2</sup>.



## Tables

**Table 1.** Experimental and DFT calculated (in parenthesis) electrochemical data of complexes **1-3** (in V vs. Fc/Fc<sup>+</sup>).

Complex	E <sub>1/2</sub> 1 <sup>st</sup> red.	E <sub>p</sub> 2 <sup>nd</sup> red.	E <sub>p</sub> 1 <sup>st</sup> ox.
<b>1</b>	-1.62 (-1.70)	-1.94	+1.03 (+1.02)
<b>2</b>	-1.67 (-1.64)	-1.98	+0.88 (+0.67)
<b>3</b>	-1.51 (-1.43)	-1.84	+0.75 (+0.58)
(bpy)Re(CO) <sub>3</sub> Cl <sup>49</sup>	-1.72 (-1.73)	-2.11	(+1.11)
( <sup>t</sup> Bu-bpy)Re(CO) <sub>3</sub> Cl <sup>17</sup>	-1.83	-2.21	

**Table 2.** Catalytic current measured at -2.16 V and corresponding computed *k* and TOF values.

Complex	<i>i<sub>c</sub>/i<sub>p</sub></i>	<i>k</i> (M <sup>-1</sup> s <sup>-1</sup> )	TOF (s <sup>-1</sup> )
<b>1</b>	6.0	50	14
<b>2</b>	4.5	28	8
<b>3</b>	7.8	84	24

**Table 3.** Functionalized electrode properties of complex **2**.

Number of CV Cycles	1	5	10	15	30
Γ (10 <sup>-10</sup> mol·cm <sup>-2</sup> ) <sup>a</sup>	~2.1	9.05	23.35	35.30	76.40
<i>i<sub>p</sub></i> in Ar (μA)	~-0.2	-4.4	-8.9	-20.1	-44.8
<i>i<sub>c</sub></i> in CO <sub>2</sub> (μA)	-45.0	-771.4	-1310.3	-1872.9	-2128.9
<i>i<sub>c</sub>/i<sub>p</sub></i>	~225.0	175.3	147.2	93.2	47.5

<sup>a</sup> Γ values are estimated with the method of charge integration from CV.